

BEHAVIOR OF TIMBER BEAMS STRENGTHENED WITH CFRP

Shengdong Zhang¹, Blanche Blondel de Joigny², Jianrong Cui³

ABSTRACT: This paper shows a study on the flexural behavior of Larch and Douglas Fir beams strengthened with Carbon Fibre Reinforced Polymers (CFRP). 60 specimens are subjected to a three-point bending test; some are reinforced only on their lower face, and others on the lower and lateral faces (U-shape reinforcement). The maximum load and the mid-span deflection at rupture lead to the determination of the mechanical properties of timber elements. A finite element analysis is proposed to complete the experimental analysis of the flexural behavior of the beams. An elasto-plastic behavior is assumed for reinforced timber and interface elements are used to model the interaction between CFRP and timber. It is observed that the predicted FE results are in good agreement with the measured test data.

KEYWORDS: CFRP, Reinforced Timber Beams, Flexural Behavior, Three-point Bending Test, FE Analysis

1 INTRODUCTION

Wood is the only renewable and most environmentally friendly construction material in the world. It has been used for ages in construction and perform well. But properties of wood are easily degraded due to its natural defects (knots, etc.) and environmentally impacts (variation of humidity, fungi, insects, etc.) on it. Reinforcements on the degraded timber members are necessitated, especially for the existing timber structures with long service time. This paper focuses on the flexural behavior of structural timber strengthened with Carbon Fibre Reinforced Polymer (CFRP).

Usually, the ruptures of bending beams are located around the knots or the other defects of the wooden pieces, or around the butt-joints next to the tensile strength. This is why they need to be reinforced in those areas to improve the tensile resistance.

CFRP is a good solution to strengthen timber elements for its high tensile strength and durability. The efficiency of the strengthening is evaluated by comparing the timber mechanical properties of the different specimens including the Modulus of Elasticity (MOE), the stiffness and the ductility of the beam, the failure modes, the resistance under bending stresses, etc. Fiorelli and Dias^[1] realized a reinforcement of small samples with G(Glass)FRP and CFRP taped on lower face. They studied the mechanical behavior of the wood under compression, then under tensile strength and then under shear, and highlighted an increase in resistance and stiffness. The defects influence is diminished.

John and Lacroix^[2] studied the effects on the length of CFRP taped on the lower face of timber beams under bending constraints. They noticed an increase of the

resistance from 40% to 70% compared to the non-reinforced specimens. They also enhanced the importance of the length of the reinforcement or to implement the reinforcement in a U-shape.

Hernandez et al^[3] investigated the bending resistance and the stiffness of glulam beams reinforced with GFRP. Three percent of the volume were added as a reinforcement, gluing two layers of GFRP on the stretched area. Some specimens were also reinforced on the top. It is noticed an increase of the resistance and the stiffness in tension: adding 3 percent of GFRP by volume increased bending stiffness by as much as 18 percent, and bending strength by as much as 26 percent. The improved efficiency of top and bottom reinforcement appears to be not significant enough to offset the added material and handling costs of two layers of GFRP, even if it enhances the beam bending strength.

Borri et al^[4] taped CFRP in the stretched zone. Some of the beams were reinforced with a prestressed reinforcement. An increase of the maximum capacity and of the stiffness compared to the other beams that were not reinforced is respectively by 22.5% to 29.2%, and by 40% to 60%. The prestressed beams do not show significant improve compared to the non prestressed ones.

Ogawa^[5] worked on the reinforcement of glulam beams made with Japanese cedar and limber pine with CFRP, around 0.08% and 1.3% of the wood volume. An epoxy resin was used to improve the shear capacity at the interface wood-carbon and the fire resistance. The bending capacity has highly increased, whatever the type of wood or the amount of CFRP used. The coefficient of the resistance variation dwindles to reach

¹ Shengdong Zhang, Department of Structural Engineering, Tongji University, 1239 Siping Road, Shanghai, 200092 China, zhangsh_d@tongji.edu.cn

² Blanche Blondel de Joigny, Department of Structural Engineering, Tongji University, 1239 Siping Road, Shanghai, 200092 China & Ecole Spéciale des Travaux

Public ESTP, Civil Engineering School, Paris, France. blanche.dejoigny@hotmail.fr

³ Jianrong Cui, Nantong Huarong Construction Group, 200 Chenggang Road, Nantong, Jiangsu, 226005 China, 1981290462@qq.com

6% to 8% compared to 10% to 25% for the non-reinforced wood.

The use of CFRP to reinforce wood structural elements is the object of more and more studies over the past decades. But we still lack a centralized data base with all the results of the literature. In this paper, the flexural behavior of Larch and Douglas Fir beams strengthened with CFRP only on their lower face, and on the lower and lateral faces (U-shape reinforcement) was experimentally and numerically studied.

2 MATERIALS AND METHODS

2.1 THE SAMPLES

60 specimens of Chinese North-eastern Larch (with mean moisture content 17.7% and density 595kg/m³) and North American Douglas Fir (with mean moisture content 13.7% and density 527kg/m³) were subjected to a three-point bending test. The size of the samples was decided according to the ASTM Standard D 143-14 "Standard methods for Small Clear Specimens of Timber" [6]. The specimens were as clear as possible, however few knots remained in some of them. The cross section is 50 mm by 50 mm, and the length is supposed to be 780 mm. The length of the beam between two supports is equal to 720 mm. This span was established in order to maintain a minimum span-to-depth ratio of 14. There are 30 specimens of each species, divided into 3 categories of 10 specimens each.

Type 1: Without any reinforcement (Figure 1-a). This group of timber specimens are the witness samples.

Type 2: With a reinforcement on the lower face of the timber beam (Figure 1-b), where wood fibers are the most solicited in bending.

Type 3: With a reinforcement on the lower face and on the two lateral faces (U shape) (Figure 1-c).

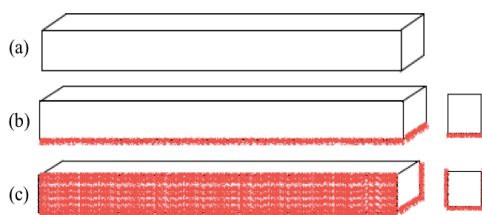


Figure 1 a-Witness Specimen, b-Reinforcement on the lower face, c-U shape Reinforcement

The carbon fibres used to reinforce the specimens have thickness 1.67mm, MOE 230000 MPa, tensile strength 3400 MPa, elongation percentage 1.7%. The taping of CFRP is parallel to the wood grain. The glue used is an epoxy resin mixed with a hardener at the ratio 1/2. A layer of 1 mm is applied 24 hours before the tapping of the CFRP sheets in order to let the resin impregnate the wooden fibers. Another layer of resin is applied just before the tapping, and a final layer above the CFRP sheet to ensure the fixing on the timber specimens.



Figure 2. Cutting and gluing the Carbon Fibers on the specimens

2.2 THE TESTING PROCEDURE

An electrohydraulic servo system was used for the destructive tests. The charge was thus applied continuously up to the specimens' failure, according to the pattern of Figure 3. The load was applied at mid-span with a speed of 5.0 mm/min. Termination of the test was at 80% of peak load of descendent stage. During the test the peak load and the load at rupture, the displacements at mid-span at the peak load and at the load of rupture were recorded for each specimen. The rupture mode was also carefully observed.

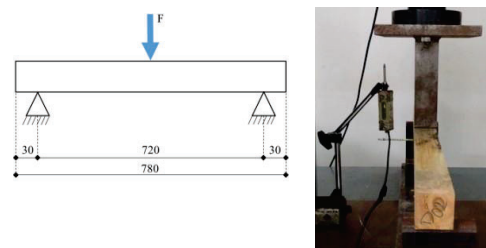


Figure 3. Disposition of the specimen on the benchmark

3 TEST RESULTS

3.1 FAILURE MODES

Larch specimens shows more flexible than Douglas Fir specimens (Figure 4) in this test.

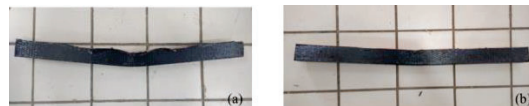


Figure 4. Larch (a) and Douglas Fir (b) reinforced beams after the test

With the same conditions of test (disposition on the benchmark, loading speed), the time before failure lasts on average 17% longer. This difference increases for the reinforced specimens, which means that the more flexible the timber is, the more efficient the CFRP strengthening is.

Except for the specimens having knots in their lower part, most of the failures occur in tension or compression. As planned, all the witness specimens

break in tension. The specimens with one face reinforced have failure most of the time in both tension and compression, or tension only. And almost all the specimens reinforced on 3 faces have failures in compression. Some wrinkles are observed on the compressive side at the point of contact between the load and the wood (Figure 5). Those wrinkles are very tiny on the witness specimens and sometimes inexistent, but on the reinforced specimens they are more important which highlights the buckling from compression strengths.

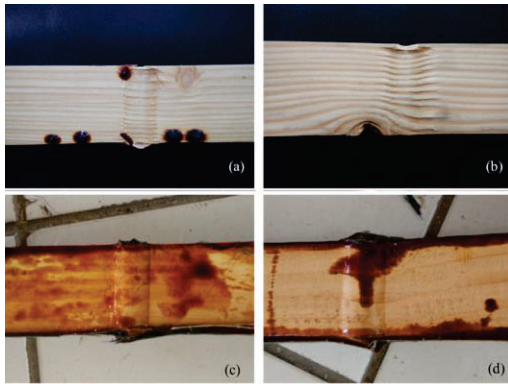


Figure 5. Buckling on compression side for the Larch specimens with one face reinforced (a, b) and for the Douglas Fir specimens with 3 faces reinforced (c, d)

3.2 LOAD-DISPLACEMENT GRAPHS

The deflection of the beams at mid-span was recorded during the tests in order to sketch the load-displacement graphs. Figure 6-Figure 11 present the results for the 60 specimens.

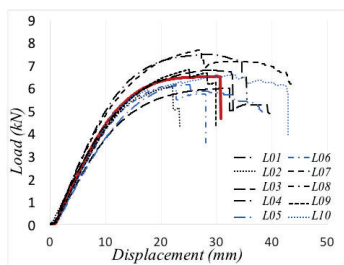


Figure 6. Load-displacement curves for Larch witness specimens

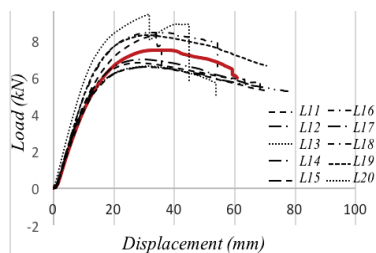


Figure 7. Load-displacement curves for Larch specimens with 1 face reinforced

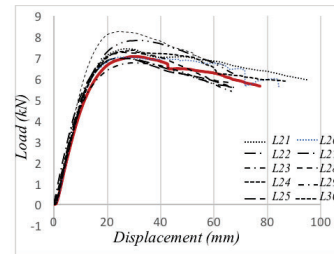


Figure 8. Load-displacement curves for Larch specimens with 3 faces reinforced

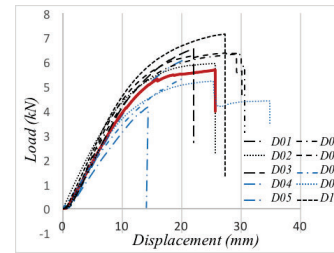


Figure 9 Load-displacement curves for DF witness specimens

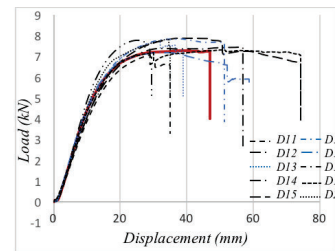


Figure 10. Load-displacement curves for DF specimens with 1 face reinforced

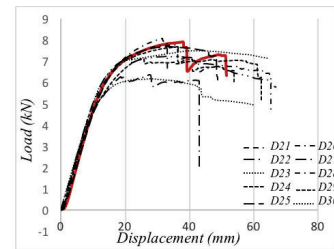


Figure 11. Load-displacement curves for Larch specimens with 3 faces reinforced

In every figure, the curve in red represents the mean of all the others; the curves in blue represent the specimens that failed because of a knot. The mean curve has been sketched removing the knot failures cases because the tests are supposed to be conducted on clear specimens according to the Standards. The analysis of the curves leads to the determination of the evolution of the MOE, and the mode of rupture of the beams. In Figure 12 the curves for Larch highlight the mechanical behavior of a timber beam: an elastic part and a plastic part are observed.

The Elastic and linear part leads to the evaluation of the MOE^[7]. Indeed, the graph equation in this first linear part is $F=k \cdot E \cdot u$ where u is the displacement, F the

measured load and k a constant. It is noticed that the slope increases significantly between the load-displacement curves of the reinforced specimens compared to the witness ones. Table 1 gives the average of all the recorded values during the tests. Those loads and displacement characteristics allow to explain the evolution of the mechanical behavior of the timber specimens. Both stiffness and ductility increase for the reinforced specimens compared to the witness ones.

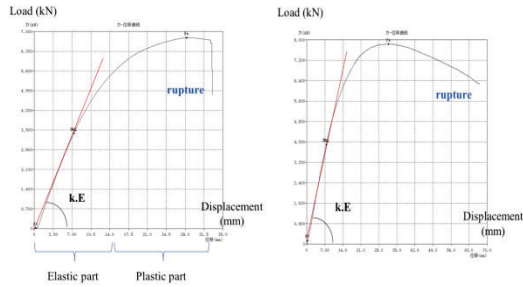


Figure 12. Load-displacement curves of Larch witness sample – rupture in tension, and of Larch with 3 faces reinforced – rupture in compression

Table 1. Average experimental values for each specimen

	Peak Load (kN)	Disp. at Peak (mm)	Load at Rupture (kN)	Disp. at Rupture (mm)
Witness DF	5,699	25,158	5,694	25,158
Witness Larch	6,548	27,874	5,855	34,559
1 CFRP DF	7,534	37,780	7,007	50,046
1 CFRP Larch	7,565	31,522	6,473	60,298
3 CFRP DF	7,356	33,325	6,286	63,819
3 CFRP Larch	7,287	27,816	6,046	74,267

3.3 LINEAR ANALYSIS OF THE MIXED SECTION

The MOE of the witness specimens was calculated with the equation of the second derivative of the deflection (Equation 1), and successive integrations gave the expression of the Modulus E_w (Equation 2).

$$E_w I_{Gz} y'' = M f_z(x) \quad (1)$$

$$E_w = -\frac{FL^3}{48y_c I_{Gz}} \quad (2)$$

where y_c = the maximum deflection at mid-span (mm), F = the peak load (kN), I_{Gz} = the section's moment of inertia (mm^4)

The computations lead to the following results:

$$E_w \text{ Douglas F} = 12\,382 \text{ MPa}$$

$$E_w \text{ Larch} = 11\,925 \text{ MPa}$$

The determination of the MOE of the mixed section (timber + epoxy resin + CFRP) is more complicated because the position of the center of gravity is modified as shown in Figure 13.

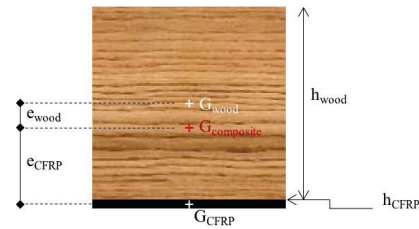


Figure 13. Position of the new neutral axis within the reinforced specimens

The bending stiffness is obtained with the theorem of Huygens (Equation 3); it will allow to be close to the reality and avoid the use of the glide factor γ pretending the bonding to be “perfect”.

$$(EI)_{eff} = E_w I_w + E_w A_w e_w^2 + E_{CFRP} I_{CFRP} + E_{CFRP} A_{CFRP} e_{CFRP}^2 \quad (3)$$

The section of the CFRP is very low so the moment of inertia I_{CFRP} can be neglected faced to the wood moment of inertia I_w . The effective stiffness is easily calculated with the (Equation 3) and the modulus of elasticity shall be obtained by dividing this value by the effective moment of inertia of the section (Equation 4) when we neglect the proper moment of inertia of CFRP:

$$I_{eff} = I_w + A_w e_w^2 + A_{CFRP} e_{CFRP}^2 \quad (4)$$

The results are presented in Table 2. The comparison with the values of $E_w \text{ Douglas F}$ and $E_w \text{ Larch}$ obtained with the witness samples shows an increase of 47% of the MOE for both species.

Table 2. Stiffness of the reinforced specimens

	$(EI)_{eff}$ kN/mm ²	I_{eff} mm ⁴	$E_w \text{ reinforced}$ MPa
DF	1.379E+7	7.536E+5	18 298
L	1.345E+7	7.635E+5	17 616

4 A NUMERICAL MODEL

4.1 Hypothesis

An elasto-plastic numerical model was introduced based on ABAQUS software. The dimensions used for the numerical modeling are $50 \times 50 \times 780$ mm for the timber beam, and $50 \times 1.5 \times 780$ mm for the CFRP reinforcement. C3D8R solid elements were used for the timber beam, and S4R shell elements for the reinforcement. The supports were fixed at 30 mm from the extremities of the samples, and the load applied at mid-span is located at 390 mm from each extremity. The wood plasticity model uses the Hill's stress

potential for anisotropic behavior^[8]. (Equation 5) gives the Cauchy stress tensor used in this model:

$$\underline{\underline{\sigma}} = \underline{\underline{\Lambda}} : \underline{\underline{\varepsilon}}^e \quad (5)$$

This elastic law was used with the mechanical characteristics of Larch and Douglas Fir taken from the table 3^[8]. The present model assumed that the behavior in the radial direction is equal to the one observed in the tangential direction. This is why the elasto-plastic model gets the following simplifications: $E_R = E_T$; $G_{RT} = G_{TR}$; $G_{LR} = G_{LT}$; $\nu_{RT} = \nu_{TR}$; $\nu_{LR} = \nu_{LT}$. The Hill's criterion was taken as yield criterion as follows, and also used as stress potential for anisotropic behaviour.

$$f(\underline{\underline{\sigma}}) = \sqrt{H(\sigma_x - \sigma_y)^2 + G(\sigma_x - \sigma_z)^2 + F(\sigma_y - \sigma_z)^2 + 2N\tau_{xy}^2 + 2M\tau_{xz}^2 + 2L\tau_{yz}^2 - R - \sigma_{yield}}$$

Table 3 Material properties for wood

Elasticity	$E_L = 14.5$ GPa	$\nu_{LR} = 0.37$	$G_{LR} = 590$ MPa
	$E_R = 1.2$ GPa	$\nu_{LT} = 0.43$	$G_{LT} = 590$ MPa
	$E_T = 1.2$ GPa	$\nu_{RT} = 0.45$	$G_{RT} = 73$ MPa
Plasticity	$\sigma_{yield} = 40$ MPa	$F = 0.35$	$L = 1.5$
	$Q = 750$ MPa	$G = 0.4$	$M = 1.5$
	$b = 17$	$H = 0.6$	$N = 1.45$

The CFRP material was considered as linear elastic orthotropic up to failure. $E_L = 110$ (GPa), $E_R = E_T = 8.82$ (GPa), $\nu_{RT} = 0.38$, $G_{LR} = G_{LT} = 4.32$ GPa, $G_{RT} = 3.2$ GPa. The surface-based cohesive behaviour was specified for modelling the adhesive interaction. For the meshing of the timber beam and the CFRP sheet, 10 for the approximate global size for seed parts was taken.

4.2 Comparison with experiments

Figure 14-figure 17 show the displacements and stresses of the modelling witness sample and reinforced sample with lower face CFRP reinforcement.

The stresses modeled in the witness specimens confirm what was observed in the laboratory during the conduction of the experiments. The stretched fibers located in the lower part of the beam are the weakest and fail first. Besides, the modelling shows the location of the neutral axis: it has not been affected at all by the bending load. For the reinforced specimens, the distribution of stresses in the stretched area is much lower than in the witness beam. This explain the high number of specimens that failed in compression more than in tension. It is difficult to conclude on the modification of the displacements of the specimens, because if the load increases so does the maximum displacement. However, the displacement itself is limited because of the presence of the CFRP sheet which reinforce the wood. The experimental results highlight a global increase of the peak load and of the displacement at rupture for the reinforced specimens compared to the witness. A comparison of the load–

deflection curves obtained from experiments and from FE analysis is made in Figure 18 for Larch specimens, and in Figure 19 for Douglas Fir specimens.

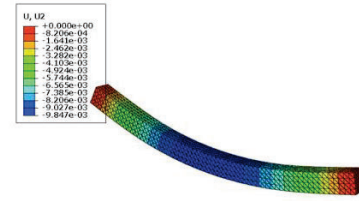


Figure 14. Displacements obtained after the modelling of the witness sample

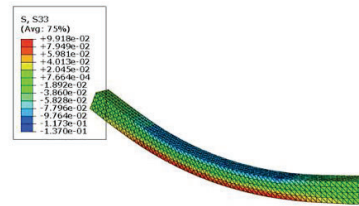


Figure 15. Bending stresses obtained after the modelling of the witness sample

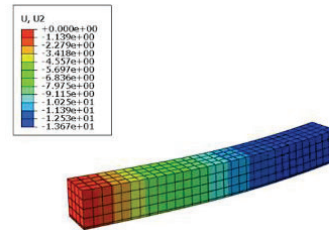


Figure 16. Displacements obtained after the modelling of half a sample reinforced along its lower face

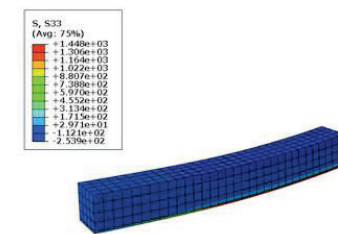


Figure 17. Bending stresses obtained after the modelling of half a sample reinforced along its lower face

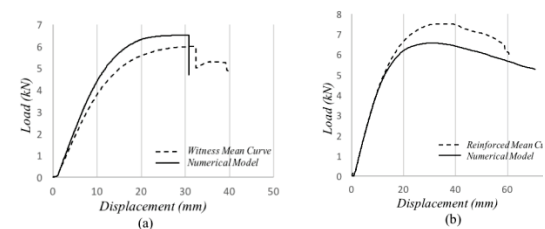


Figure 18. Larch load–mid-span deflection curves: comparison between numerical and experimental data (a)–

witness and (b)-reinforced specimens

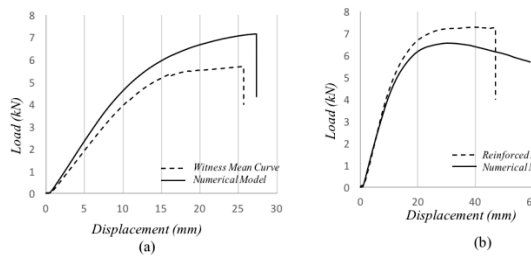


Figure 19. DF load-mid-span deflection curves: comparison between numerical and experimental data (a)-witness and (b)-reinforced specimens

For the Larch's witness specimens, the behavior obtained with the FE analysis is linear up to a displacement of about 10 mm with a corresponding load that reached 4.5 kN, before entering in the plastic behavior. The witness mean curve has an elastic zone up to a displacement equal to 7.8 mm and a load of about 3.5 kN. Beyond those points the response became nonlinear and a discrepancy between predicted and experimental results was observed. The peak load is reached at rupture for the numerical model, and is about 6.5 kN for a maximum displacement of 30.4 mm. Whereas the experimental data lead to a peak load that does not correspond to the failure one, even if it is close to prediction of the FE model: 5.8 kN for a displacement of about 32 mm. However, the rupture occurs at the ultimate load of 5.3 kN with a displacement that reaches 39 mm. The comparison between the numerical and experimental data about reinforced specimens on the lower fibers also show similitudes in the elastic area and divergence in the plastic area. The behavior is linear up to a displacement of about 9.6 mm with a corresponding load of 4 kN. The plastic stage lasts longer in the FE simulation: ultimate displacement is equal to 73 mm for an ultimate load that reaches 5.3 kN. The experiments show a mean final displacement up to 58 mm with a corresponding load of 6.5 kN, and a rupture in both compression and tension (sudden drop of the load for constant displacement visible on the curve).

For the Douglas Fir's witness specimens, the FE analysis shows a linear behavior up to a displacement of about 9 mm with a corresponding load of 4.1 kN, before the plastic stage. The elastic zone of the mean curve goes up to a displacement of 10 mm with a load of about 3.8 kN. The rupture is similar between the experimental and the numerical results: it is sudden and typical of a tensile failure. The experimental rupture occurs for an ultimate load of about 5.4 kN and a maximum displacement of 25.5 mm, whereas the numerical model shows a rupture for a load equal to 7.2 kN and a displacement that reaches 27 mm. As for Larch specimens, the comparison between the numerical and experimental models shows similitude in the elastic area. The slopes of the curves are very close, and the behavior is linear up to a displacement of about 8 mm with a corresponding load of 3.2 kN. Once again,

the plastic stage lasts longer for the FE simulation. The maximum displacement is about 60 mm and the ultimate load reaches 5.8 kN, whereas the plastic stage of the experimental results is shorter. The rupture mode is different because the curve shows a tensile rupture with a load that drops suddenly from 7 to 4 kN for a corresponding displacement of about 44 mm.

The comparison of the load-displacement curves of the reinforced specimens is surprising, because the peak load seams to decrease from the witness results to the reinforced scheme. This means that the numerical model is not close enough to the reality in the plastic area. The FE model shows an improvement of the ductility of the specimens because the final displacement increased a lot compared to the witness one. But the improvement of the specimens' stiffness is not obvious according to the numerical modelling. However, we can notice that the curves are close enough in the linear part to validate the numerical model as far as the elasticity of the wood is concerned.

5 CONCLUSIONS

The experiments conducted on the specimens of Larch and Douglas Fir and the numerical modelling allowed to reach the following conclusions:

- (1) CFRP reinforcement increases the load carrying capacity of the specimens. The peak load of the Douglas Fir witness specimens is around 5.7 kN and reaches 7.5 kN for the reinforced specimens. For Larch witness specimens it is around 6.5 kN and reaches also 7.5 kN for the reinforced specimens. The MOE increased by 47 % for both Douglas Fir and Larch specimens with CFRP reinforcement.
- (2) CFRP reinforcement improves the ductility of the timber specimens. The maximum displacement at rupture is much higher for the reinforced specimens than for the witness specimens.
- (3) The U-shape reinforcement has no significant impact compared to the single one-layer reinforcement of the lower fibres as far as load carrying capacity is concerned, but significant impact compared to the single reinforcement of the lower fibres as far as ductility is concerned.
- (4) The failure mode changes with reinforcement. Witness specimens fail in tension. Some specimens which had their 3 faces reinforced had their rupture in compression, others in compression coupled with tension, and few of them had their rupture at their defect's localization (knot).
- (5) The Numerical model can be validated for the elastic behavior of the wood, but not for the plastic behavior. Even if the ductility is indeed improved, the maximal load carrying capacity decreases between the reinforced specimens and the witness which is the opposite observed during the experiments. The combination of the failure modes and the compressive failures both perpendicular and parallel to the grain can explain this difference.

6 DISSCUSSION

Several improvements can be proposed in order to maximize the efficiency of the CFRP reinforcement.

(1) The experimental results showed that the U-wrapping of the beam with the Carbon fibers sheet delays the rupture by improving the ductility of the specimens, but does not improve the stiffness. Indeed, on the lateral faces only the wood fibers located below the neutral axis work in tension, the others are subjected to compression. For beams with bigger sections, the U-shape reinforcement could cover only half of the lateral face. This new reinforcement design would diminish the costs of the CFRP used for the reinforcement.

(2) The section of CFRP stayed constant during the whole experiment. An increase of the thickness of the carbon fibers sheets or the taping of several layers could improve the reinforcement. A study was led by Borri et al^[4], where the efficiency of the reinforcements with one, two and three layers of CFRP were compared. Three sheets of CFRP resulted on a 60% increase of the flexural strength.

(3) The timber species has an impact on the testing results. Sometimes, CFRP reinforcements concern the renovation of old buildings built with oak or chestnuts. Those species have tyloses which can block pores. This feature allows the protection of wood against moisture so it can have an impact on the impregnation of the resin. Thus we obtain very thin adhesive film thicknesses, but it may not be quite adherent to the support. Besides for very thin film, the ambient humidity has an influence on the epoxy resin and may weaken it.

ACKNOWLEDGEMENT

The authors would like to thank the two companies who provided the materials for conducting the experiments Shanghai Yichang Carbon Fabric Materials Co., Ltd for the Carbon Fibers, and AONA Wood Structures for the timber specimens.

REFERENCES

- [1] Fiorelli J. Dias AA. Analysis of the strenght and stiffness of timber beams reinforced with carbon fibre and glass fibre, *Material Research* 6, 193-202, 2003.
- [2] John KC. Lacroix S. Composite reinforcement of timber in bending, *Canadian Journal of Civil Engineering*, 27, 899-906, 2000.
- [3] Hernandez R. Davalos JF Sonti SS. et al. Strength and stiffness of reinforced yellow-poplar glued-laminated beams. US Department of Agriculture, Forest Service, Forest Product Laboratory, 1997.
- [4] Borri A. Corradi M. and Grazini A. A method for flexural reinforcement of old wood beams with CFRP materials. *Composite: Part B – Engineering*; 36:143–53, 2005.
- [5] Ogawa H. Architectural application of carbon fibers, development of new carbon fiber reinforced glulam. *Carbon* 38, 211-226, 2000
- [6] American Society for Testing and Materials (ASTM). Standard methods for Small Clear

Specimens of Timber, ASTM D 143-14. Annual book of ASTM standards. ASTM, West Conshohocken, Philadelphia, 1995.

- [7] Tingley DA, The stress-strain relationships in wood and fiber-reinforced plastic laminate of reinforced glued-laminated wood beams, PhD Dissertation, Oregon State University, Corvallis, 1996.
- [8] Khelifa M. et al. Finite Element analysis of flexural strengthening of timber beams with Carbon Fiber-Reinforced Polymers, *Engineering Structures* 101, 364–375, 2015.